Desalination and Water Treatment
www.deswater.com
doi: 10.5004/dwt.2023.29515

293 (2023) 43–48
May

Computational fluid dynamics calculations of high efficiency heat exchangers operating in laminar motion consisting of extruded plastic profiles with inserts

Mario Vismara[a,*], Nicolò Mazzetti[b], Riccardo Mereu[b]

[a]*Via Lavoro 5, 23880 Casatenovo (LC), Italy, email: mariovisma@tiscali.it*
[b]*Department of Energy, Politecnico di Milano via Lambruschini 4a, 20156 Milano, Italy, emails: nicolo.mazzetti@polimi.it (N. Mazzetti), riccardo.mereu@polimi.it (R. Mereu)*

Received 20 October 2022; Accepted 16 March 2023

ABSTRACT

The use of plastic-based materials is finding new applications in the heat exchangers sector: the very high values of heat exchange surface ratio per volume unit, the lightness of the products and the lower cost achievable with plastic material are the main advantages of resorting to their use (1),(2),(3). The object of this study is to analyze and validate in terms of CFD and thermodynamic analysis a solution for the realization of high efficiency counter-flow heat exchanger (HX) consisting of extruded alveolar/multi-wall polycarbonate profiles with inserts. Bundles composed of multiple channels are commonly produced to form alveolar/multi-wall polycarbonate products/panels; several extruded bundles can be assembled to obtain HX with large sections, making it possible to require shorter paths for the fluids and lower speed of the same, and therefore less pressure losses in pumping. A further characteristic of the HX analyzed is that, in order to obtain high values of thermal power per unit of volume, instead of resorting to pumping of fluids in turbulent motion, which is an energetically very expensive solution, this result is achieved thanks to the introduction, inside of the little channels that make up the extruded bundle, of filling profiles; those filling profiles produce a reduction in the passage thickness of the fluids and induce some positive effects on the nature of their motion: this leads to an enormous improvement of the value of the HX power per unit of surface. Six different CFD calculations were carried out with counterflows of 25 $m^3/h \cdot m^2$ of water at inlet temperatures of 20°C and 100°C with square channels of 1 meter in length, 8 mm side and three different fillings, obtaining high volumetric heat transfer coefficient (in the cases examined up to 615 $kW/m^3 \cdot K$) and low pressure drops.

Keywords: Counter flow heat exchangers; Extruded plastic bundles; Laminar motion; CFD analyses

1. Introduction

On the market there are numerous types of extruded multi-wall panels in polycarbonate (or other plastic materials), usually designed to form windowed walls with high insulating power (Fig. 1). In fact, the extruded alveolar structure not only provides a light but mechanically robust product, but it also shows its internal spaces divided into a high multiplicity of layers of channels, separated by a very thin plastic film, a feature that greatly improves the insulation capacity. In some commercial products the thickness of the walls of the channels is less than 0.035 mm and however the presence of frequent transversal parts (a common mesh of the extruded products on the market is that made up of channels with a section of 2.5 mm × 8 mm) gives them considerable mechanical resistance.

The most common characteristics of the products on the market can be deduced from the observation of Fig. 1: as can be seen, the structure is made up of channels, generally with a rectangular section, however it is easy to deduce

* Corresponding author.

the possibility of producing extruded bundles which have almost any type of preferred structure.

The idea analyzed in this study is to use the innumerable channels that constitute the extruded bundle and which, given the extrusion technique, can have a discretionary length, to exchange heat and constitute a counter-flow heat exchanger; this can be done by feeding the channels with the hot and cold flows arranged in a checkerboard pattern (preferable solution for extrusions with square section channels) or arranged by interposed layers (preferable solution for extrusions with rectangular section channels). In order to efficiently feed and discharge fluids, a solution has been studied and found that allows, in a sufficiently simple way, not only to be able to feed and drain fluids from and into all the numerous channels of a bundle with a single feed, but also to repeat this process and unify the feed socket and purge to a plurality of side-by-side extruded bundles, thus creating a bundle of extruded bundles fed and purged from a single feed and purge opening (depicted in Fig. 2). This last opportunity is extremely important as it allows to increase the overall section of the HX almost at will in order to arrange the flow of fluids in the channels at a desired speed, to reduce the length of the channels and therefore also the drop in pumping pressure and so the pumping energy required.

From the point of view of thermal conductivity, as it is known, plastics have much lower values than those of metals; to be competitive, this disadvantage must be compensated with lower costs and by the possibility of offering much higher exchange surfaces per unit of volume and very low thicknesses of the channel walls. It should also be noted that plastics are not suitable for use in turbulent flow to enhance heat exchange efficiency. This is because turbulent flow requires high pumping pressures, which are both energy-intensive and require a sturdy structure that plastics cannot provide, especially with reduced thickness or at high temperatures.

Moreover, operating with the alveolar beams described above with laminar flow field, we would encounter the problem that the minimum internal dimensions of the channels obtainable with the current extrusion technology are too large to allow interesting values of thermal power per unit of volume. The solution to this problem is the object and the peculiarity of this study, that is to analyze by means of CFD simulations the possibility of improving the heat transfer coefficient by introducing fillings inside the channels which:

- first of all reduce the thickness that is free to the passage of the fluids;
- by slowing down the speed of the portion of flow farthest from the heat exchange surface, they further improve the ratio between the ΔT which promotes the heat exchange and the logarithmic mean temperature difference (LMTD) between the two flows.

Fig. 3 shows an exemplary front section of nine square-section channels and the filling. Note the presence on the central body of the filling of protuberances that perform the following functions: the central ones support the thin diaphragm film to better resist the pressure differences

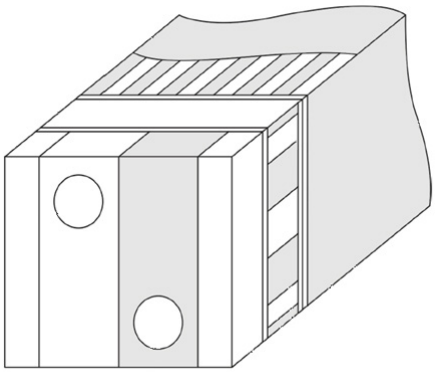

Fig. 2. Illustration of a proposed solution for unifying the feeding and purging of several counterflow channels of an extruded bundle.

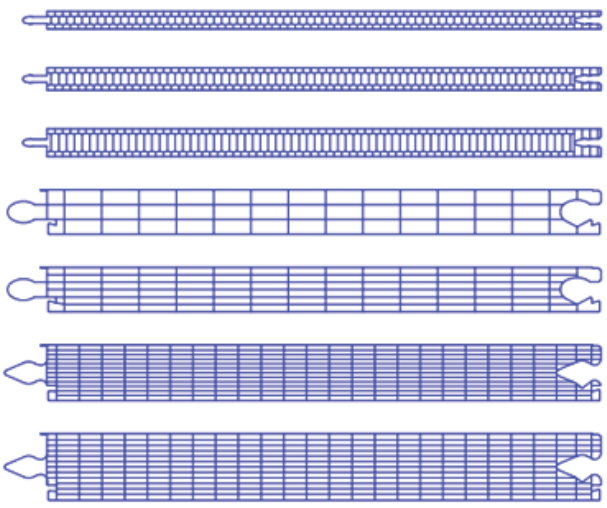

Fig. 1. Examples of extruded polycarbonate multi-wall panels commercially available (4).

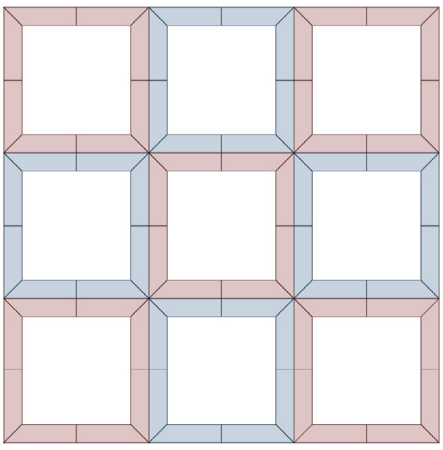

Fig. 3. Front view of a part of a bundle consisting of 9 channels operating with checkerboard counterflows.

that occur along their path between the counterflows of adjacent channels, while those in the corners, in addition to determining the centering of the filling, have the function of slowing the speed of the flow in an area not favored in thermal exchanges; in their absence, the greater opening to the passage of fluids and therefore the less resistance at their passage and their greater relative speed would entail a negative effects on the efficiency of the HX.

Note that for the purpose of calculating the heat exchange, the CFD analysis of a single portion of two adjacent channels is sufficient (a section of the computational domain is reported in Fig. 4) since only the central wall participate in the heat exchanges and therefore, being all the other adiabatic walls, the flow is not influenced by other thermal inputs; furthermore, all portions of the channels that make up the beam are absolutely symmetrical or equal.

The calculations were carried out on three different configurations of a channel of 1 m in length having the side of 8 mm with a free thickness at the passage of the fluid of 0.2, 0.3 and 0.1 mm, identified from now on as configuration 1, 2, and 3, respectively. The thickness of the rostrums protruding from the filling used in the calculations is 0.3 mm, the one of the film-diaphragm is 0.072 and 0.036 mm depending on the case considered. The two counterflows consist of water at the respective temperatures of 20°C and 100°C and have an identical flow rate of 0.2 L/h for the portion of the channel examined (i.e., one eighth of the channel section); the heat exchange surface area of the portion is 3.6–0.3 m^2 which accounts for 225.1 m^2/m^3.

2. Numerical modelling

The grid used for the study is made up of about 4 million regular hexahedral elements, with mesh refinement in proximity of the walls and the membrane. The mesh features have been defined to obtain a grid fine enough to capture and solve all the domain details. In addition, the use of the second-order discretization scheme and the adoption of RANS models give the numerical model an overall accuracy adequate to predict the values of the desired quantities.

The modeling tool used is the CFD software ANSYS-Fluent 2021 R2. As described in the introduction paragraph, a laminar flow is completely solved with mass balance, Navier–Stokes and energy balance equations. No other equations are needed, and no further model is required. Considering an incompressible flow, the above-mentioned equations result as follows:

$$\nabla \cdot \left(\bar{v}\right) = 0 \tag{1}$$

$$\rho \bar{v} \cdot \nabla \bar{v} = -\nabla p + \nabla \cdot \left(\bar{\bar{\tau}}\right) \tag{2}$$

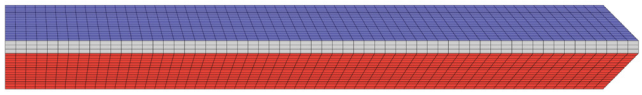

Fig. 4. Mesh detail: red and blue colors indicate the two counter-current channels while the grey region corresponds to the membrane film.

$$\nabla \cdot \left(\rho \bar{v} c_p T\right) = \nabla \cdot \left(k \cdot \nabla T\right) \tag{3}$$

The algorithm chosen to solve the set of equations is the "segregated solver" (pressure-based) with implicit formulation. Using this approach, the equations are solved sequentially. Since the equations are nonlinear (and coupled), it is necessary to perform several iterations of the solution cycle before obtaining a converging solution.

The simulation was performed in a steady-state motion- and Green–Gauss Node Based method was used for gradient discretization. The pressure-velocity coupling was handled using the Coupled (pseudo-transient active) method. The spatial discretization was achieved using PRESTO! for pressure and Second-Order UPWIND for other equations, providing a balanced and efficient solution to the transport equations.

Specific boundary conditions that describe the behavior of the system at the inlets, outlets, walls, and membrane have been imposed. At the inlets, a mass flow rate of 0.2 L/h was imposed in each channel, with a temperature of 20°C for the cold side and 100°C for the hot side. The output was defined by an imposed static pressure equal to the ambient pressure. The walls were modeled as stationary with no slip condition and adiabatic, while the membrane was modeled as non-slip wall with zero mass flow and a thermal conductivity set to 0.2 W/(m·K).

3. Results

Global results for the main variables of interest are summarized below for the analyzed configuration in terms of pressure drops and exchanged power. Table 1 reports the results obtained from the simulation that considered the membrane thickness equal to 0.072 mm, while in Table 2 the membrane thickness is considered as 0.036 mm.

The tables report the temperature of the fluid leaving the system on both cold and hot side, as well as the pressure drops across both channels, the logarithmic mean temperature difference, the thermal power transferred by the system and the heat transfer rate per unit of volume.

As expected, the third configuration allows for the highest heat transfer with the drawback of having also the highest pressure drop. Looking at the figures shown in the tables above, it seems to be the least attractive geometry for the purpose of this work. Indeed, comparing the results of the three cases, the latter results in a 1.5% increase in power exchanged compared to the second configuration in face of pressure drop more than twenty times higher. The other two geometries face a better trade-off between exchanged power and pressure drops.

In a second phase, the results obtained from the numerical simulations were compared with values obtained from empirical correlations. In particular, the value of the overall heat transfer coefficient between the two fluid channels was compared. In all configurations, given the particular geometry of the channels, the Nusselt number suggested by the literature is approximated to that corresponding to the case of parallel flat plates and equal to 5.39(5). From this, the convective heat transfer coefficient was derived, considering a hydraulic diameter of $D\_h = 4 \times A/p$ and at the end

the conductive resistance has been summed with the convective ones obtaining the total resistance which is the reciprocal of the heat transfer coefficient. The same heat transfer coefficient has been derived from the numerical results through the following formula:

$$U_{tot} = \frac{P}{\text{LMTD} \cdot S} \tag{4}$$

where P is the exchanged power between the two channels; S is the heat exchange area.

Table 3 shows the numerical values of the above-mentioned quantities. It can be noted that the deviation decreases with the increasing aspect ratio of the channels, in accordance with the hypothesis of flat plates seen previously.

The value of the heat exchange coefficient per unit of volume indicated above does not refer to the entire HX but only to its portion consisting of the channels; therefore it does not vary with the length of the ducts, while, if reference is made to the heat exchange value of the entire HX structure, it is necessary to take into account the space occupied

Table 1
Results comparison between the different geometrical configurations considering a membrane thickness of 0.072 mm

	Configuration 1	Configuration 2	Configuration 3
Outlet temperature cold side (°C)	96.99	96.37	97.60
Outlet temperature hot side (°C)	23.01	23.63	22.40
Pressure drophot side (Pa)	12,573.51	3,850.62	97,318.46
Pressure dropcold side (Pa)	13,189.06	4,074.85	101,202.43
LMTD	3.01	3.63	2.40
Thermal power (W)	17.86	17.71	18.00
Heat transfer rate per unit of volume (MW/m^3)	1.116	1.107	1.125

Table 2
Results comparison between the different geometrical configurations considering a membrane thickness of 0.036 mm

	Configuration 1	Configuration 2	Configuration 3
Outlet temperature cold side (°C)	97.88	97.26	98.49
Outlet temperature hot side (°C)	22.12	22.74	21.51
Pressure drophot side (Pa)	12,725.87	3,897.22	98,475.52
Pressure dropcold side (Pa)	13,148.33	4,062.41	100,865.61
LMTD	2.12	2.74	1.51
Thermal power (W)	18.06	17.92	18.20
Heat transfer rate per unit of volume (MW/m^3)	1.129	1.120	1.138

Table 3
Comparison between global heat transfer coefficient derived from analytical equations and resulting from numerical simulation

	Configuration 1	Configuration 2	Configuration 3
h (W/m^2·K)	9,182.90	6,327.92	17,765.21
U_an (W/m^2·K)	1,730.71	1,479.16	2,116.05
U_CFD (W/m^2·K)	1,647.36	1,355.86	2,081.21
Numerical error (%)	–5%	–8%	–2%

Table 4
Results from simulations with both meshes

	Mesh A	Mesh B	Δ%
Outlet temperature cold side (°C)	97.5993	97.5993	0.00002%
Outlet temperature hot side (°C)	22.4007	22.4008	–0.00013%
Pressure drophot side (Pa)	97,318.46	97,322.98	–0.00464%
Pressure dropcold side (Pa)	101,202.43	101,208.64	–0.00614%

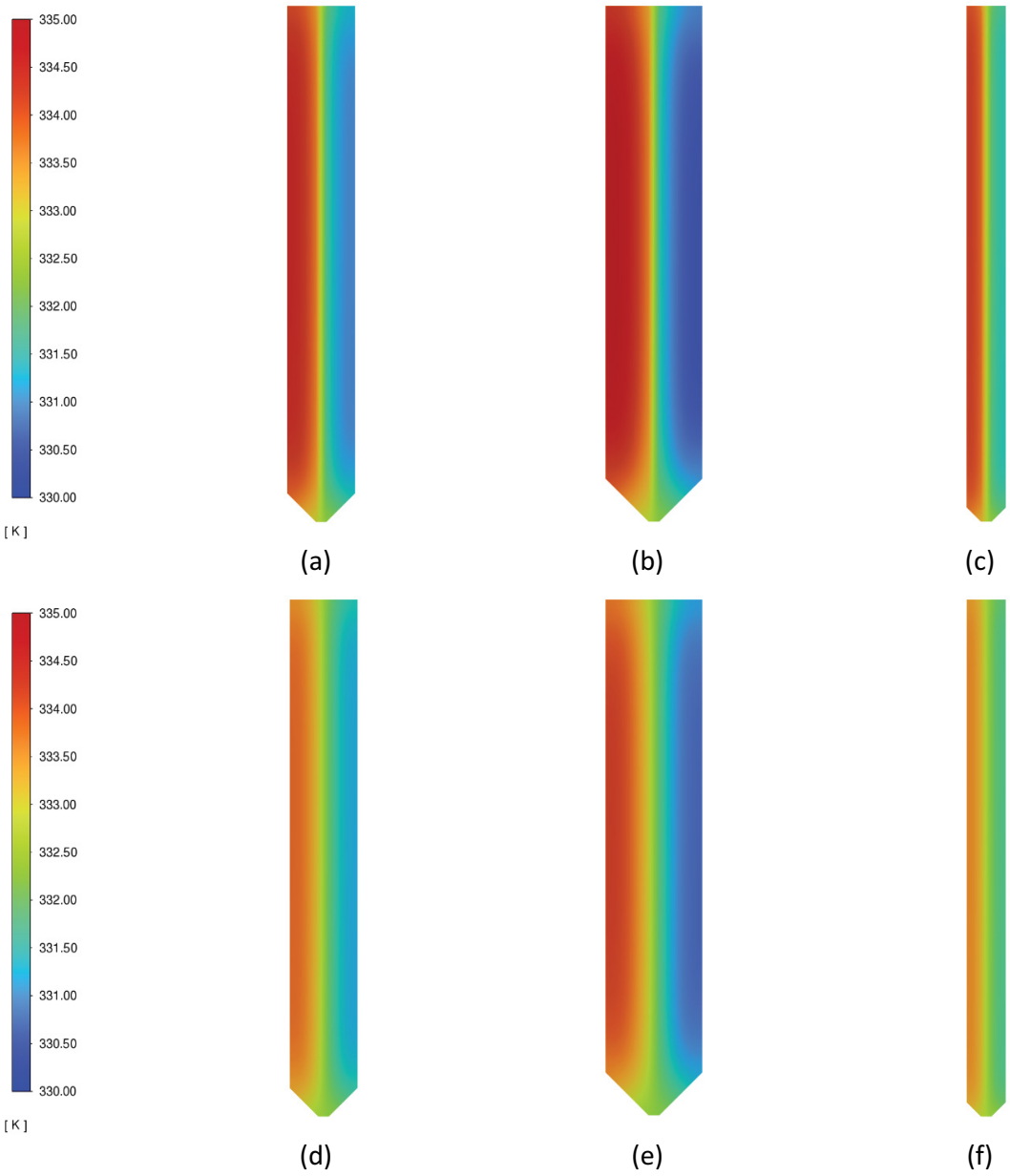

Fig. 5. Temperature distribution in the section located at half of the hx length. (a–c) refer to the case in which the membrane thickness is 0.072 mm, respectively for configuration 1, 2, and 3. (d–f) are referred to the simulations in which the membrane thickness is 0.036 mm, in the same configuration order as above.

by the supply/purge connection structure which, depending on the size of the designed section, will require an additional depth varying from 20 to 30 cm approx. Given its greater section of passage of fluids, the connection structure involves only a negligible drop in pumping pressure.

As last step, a grid sensitivity analysis has been performed considering the geometry of the configuration 3 with a membrane thickness of 0.072 mm. Two different grids have been tested; the first one (mesh A) has about four million elements while the other (mesh B) has roughly eight million cells.

From Table 4 it can be noted that there are no relevant differences between the results of the simulations with two different grids. Thus, we can conclude that the results are not influenced by the mesh characteristics.

4. Conclusion

The study carried out and reported here aims to demonstrate the possibility of reaching extremely high values of thermal power per unit of volume with structures as described above at the same time as with extremely low pumping values and structural costs.

The excellent values found indicate that the HX identified in the study could find interest in various applications, among the others:

- the heating of the water supplying the swimming pools which, according to the legislative provisions, in the public ones must be replaced daily for at least 5% of their volume;
- MVC desalination technology which requires very efficient HX with low pumping pressure drops.

It should be noted that beyond what has been examined in this study, it is probable that the excellent results achieved will also be replicated by modifying the profile and characteristics of the fillings of the channels which can thus validly perform various other functions.

References

[1] C. Legorreta, J.B. Tonner, Steen Hinge, Plates – the next breakthrough in thermal desalination, Desalination, 134 (2001) 205–211.
[2] G. Micale, L. Rizzuti, A. Cipollina, Eds., Seawater Desalination Conventional and Renewable Energy Processes, Springer, Berlin, Heidelberg, 2009.
[3] A.R.J. Hussain, A. A. Alahyari, S.A.Eastman, C. Thibaud-Erkey, Review of Polymers for Heat Exchanger Applications: Factor Concerning Thermal Conductivity, University of Massachusetts Lowell, 2016.
[4] https://www.akraplast.com/images/prodotti/Akrapan_UV_R14_IT.pdf
[5] W.M. Kays, M.E. Crawford, Convective Heat and Mass Transfer, 3rd ed., McGraw Hill, New York, 1993.